Interaction effects in the many-valley system of Si MOSFET's

J. Lutz and F. Kuchar
Institute of Physics, University of Leoben A-8700 Leoben, Austria

(Received 28 May 1996; revised manuscript received 25 September 1996)

The interaction of the electrons in Si MOSFET's has been studied under uniaxial stress using quantum-magnetotransport experiments (Shubnikov–de Haas and quantum-Hall effect). The stress allows us to vary the relative positions of the conduction-band valleys where the electron-electron interaction plays a crucial role. From the evaluation of the data we obtain the phase diagram of the population of the valleys as a function of stress and carrier density. Our results are excellently described by the theory of Takada and Ando where intervalley electron-electron interaction is taken into account. As regards the problem of the valley degeneracy g_v, conditions can be established under stress where the interplay of stress and electron-electron interaction allows $g_v > 2$, not observed before in transport experiments. [S0163-1829(97)00704-2]

I. INTRODUCTION

Beyond the independent-electron approximation, interaction effects play an important role in semiconductors. The interaction of electrons in different valleys in k space can be studied in a many-valley semiconductorlike silicon. This is particularly interesting in the two-dimensional electron system (2DES) of an n-channel silicon MOSFET where the relative positions of the valleys can be varied by the application of an external parameter like uniaxial stress. Much attention was paid to the study of Si MOSFET's already at the beginning of the physics of 2DES.[1] Experimental investigations concerned magnetotransport,[2] piezoresistance,[3] and cyclotron resonance measurements.[4] Theoretically, essentially two models were developed. The one of Kelly and Falicov[5] was based on charge-density waves (CDW's) resulting from phonon-mediated intervalley electron exchange interaction. Takada and Ando[6] and also Stern and Howard[7] considered the interaction without involving phonons. The CDW model was initially supported by the observation of a single cyclotron resonance (CR), which varied in position continuously between the two masses of the valleys when varying their relative populations. According to the Takada-Ando model the observation of two cyclotron resonances was expected. Results of Shubnikov–de Haas (SdH) experiments could never be uniquely interpreted in favor of one of the two models. Eisele, Gesch, and Dorda[8] preferred the CDW interpretation, Englert *et al.*[9] doubted that the electron-phonon interaction was strong enough for the occurrence of CDW's. Subsequent CR experiments[10,11] revealed the existence of two cyclotron masses under conditions where two valleys were expected to be populated. This agreed with the Takada-Ando model. However, in SdH experiments also performed by Gesch, Dorda, and Stallhofer[12] a constant SdH period was observed when varying the stress. Thus, the understanding of the interacting 2D electron system in silicon, the prototype many-valley semiconductor, was far from being satisfactory.

In the present work, Si MOSFET's of (001) orientation have been studied under uniaxial stress using high-magnetic-field experiments, i.e., evaluating the SdH effect and the quantum-Hall effect. The results allow us to establish a phase diagram of the population of the valleys involved. Also information on the valley degeneracy is obtained from the data.

II. THEORETICAL BACKGROUND

A. The stressed Si(001) MOSFET

The projection of the constant energy surfaces of the Si conduction band onto a (001) plane yields two circular and four elliptical energy contours.[1] In a 2DES confined in the z direction by a triangular potential the energetic positions of the valleys are determined by $(m_z)^{-1/3}$, m_z being the effective mass in the [001] direction. This means that the [001] valley with $m_z = m_l$ (m_l is the longitudinal mass) is lowest in energy and with valley degeneracy $g_v = 2$. The application of uniaxial stress causes shifts of the valleys. This is calculated according to Refs. 13 and 14 and shown schematically in Fig. 1 for two directions of compressive stress.

B. Interaction effects

Intervalley electron interaction was treated theoretically essentially in two ways.[5,6] Takada and Ando[6] took the interaction into account within the Hartree, Hartree-Fock, and random-phase approximations. Their results are shown in Fig. 2 for compressive stress in the [100] direction, i.e., in the plane of the 2DES parallel to the long axis of two of the elliptical valleys. Generally, the effect of the electron-electron interaction is to cause a gradual change of the population of the lowest valleys ([100] or [001]) with a mixed phase between $n_{001}/n_s = 0$ and 1. n_s is the total electron density, n_{001} the one in the [001] valley. The width of the mixed phase and its onset with respect to a variation of n_s or X depends on the approximation applied. In the Hartree approximation the Coulomb interaction of the electrons with a background charge, which includes the other electrons, the depletion charge, and the image charge, is considered. The change of the population is always gradual also for small n_s values. The Pauli principle, taken into account in the Hartree-Fock approximation, weakens the repulsive force of electrons with the same spin and valley index by keeping them apart. Being in different valleys (in k space) the elec-

0163-1829/97/55(4)/2315(6)/$10.00 © 1997 The American Physical Society

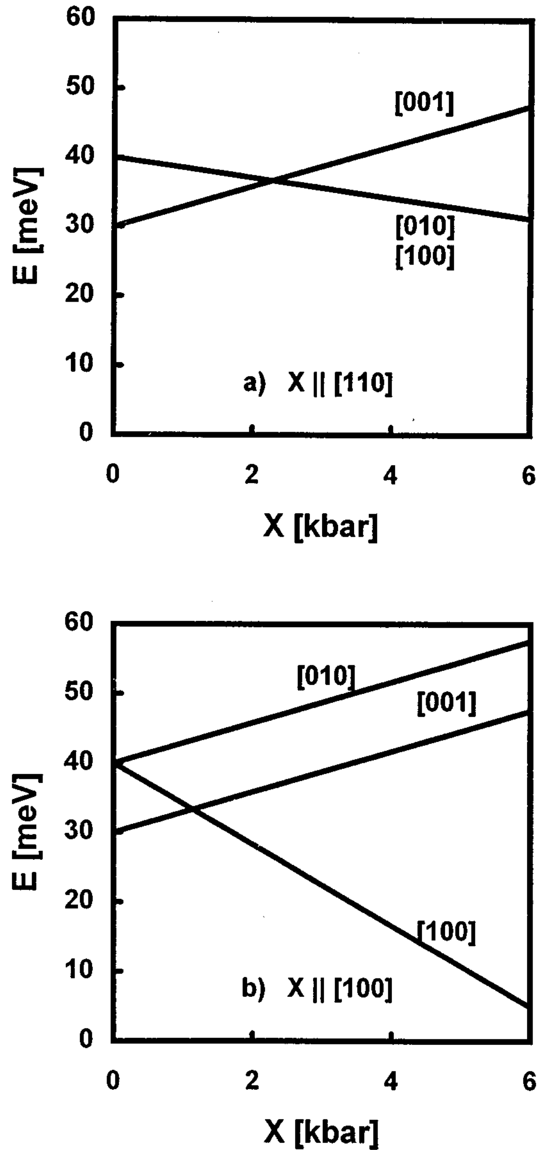

FIG. 1. Energetic positions of the valleys in a (001) Si MOSFET for different stress directions without electron-electron interaction. (a) $X\|[110]$; (b) $X\|[100]$.

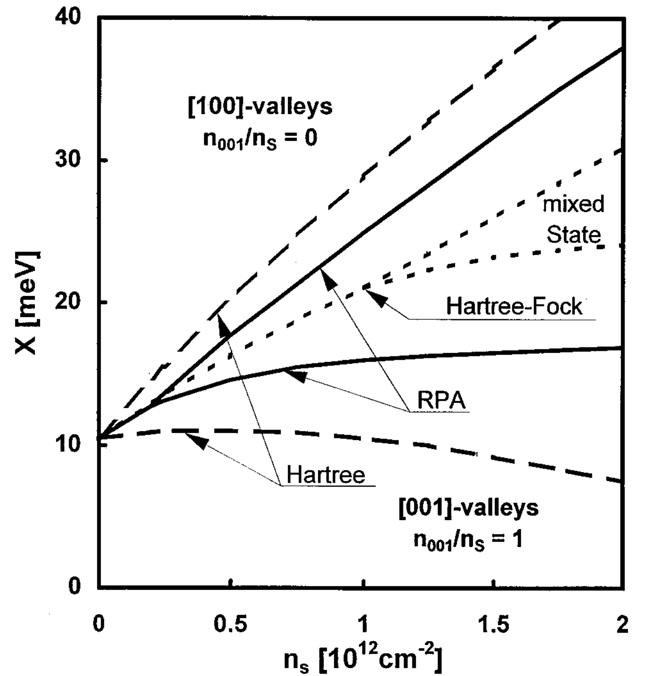

FIG. 2. Theoretical phase diagram of an n-channel inversion layer on a Si(001) surface under uniaxial compressional stress in the [100] direction after Takada and Ando, $n_{\mathrm{dep}}=2.23\times10^{11}$ cm^{-2} (Ref. 6). The conversion factor of X from kbar (Fig. 1) to meV is 8.8 meV/kbar.

trons could be closer in real space. This would increase their energy. Therefore, it is energetically favorable for the electrons to be in the same valley. Compared to the Hartree results, this exchange effect causes a tendency towards an abrupt change of the population at low densities n_s. Beyond the exchange interaction of the Hartree-Fock approximation the random-phase approximation (RPA) includes the higher-order correlation contributions. The effect of correlation is to make electrons in the occupied valleys move more dynamically so avoiding the electrons in the unoccupied valleys. This reduces the exchange effect and lowers the energy of the unoccupied valleys. In Fig. 2 this is reflected by the shift of the onset of the mixed phase to lower n_s values. Kelly and Falicov's treatment[5,15] showed that the phonon-mediated coupling between the valleys leads to the formation of a CDW state (between $n_{001}/n_s=1$ and 0) if the intervalley interaction is sufficiently strong. However, for fitting experimental data Kelly and Falicov had to assume an extremely large Coulomb repulsion. A consequence is that with increasing stress a discontinuous first-order phase transition takes place near $n_{001}/n_s=1$ and a second-order transition near $n_{001}/n_s=0$. In contradiction to these results Kelly and Hanke[16] found the effect to be too weak for the formation of CDW's.

III. EXPERIMENTAL ARRANGEMENT AND SAMPLES

Silicon (001) MOSFET's with standard Hall bar geometry were used. Length and width were 800 and 80 μm, respectively. Two potential probes on each side were spaced by 160 μm. The thickness of the gate oxide was 680 nm. At $T=2.1$ K the maximum electron mobility was 2×10^4 cm^2/V s (at $V_G=10$ V). The long axis of the MOSFET was oriented in the [110] direction. The long axis of the sample, i.e., the stress direction was either [100] or [110]. The total size of the sample was $6\times2\times0.5$ mm^3 ([100] sample) and $6\times1\times0.5$ mm^3 ([110] sample). For the electrical contacts 25-μm-diameter gold wires were bonded to the aluminum pads of the MOSFET.

For the magnetotransport experiments under uniaxial stress the samples were mounted in a holder where the stress was applied in the plane of the 2DES and perpendicular to the magnetic field. The force was applied by stainless-steel strings via pulleys (see Ref. 17). For applying the force uniformly and for isolating the sample electrically, Mylar foils were positioned between the sample and the pistons of the stress apparatus. The maximum stress that could be produced was 2.5 and 6 kbar in the samples with $X\|[100]$ and [110], respectively. The stress was determined from the external

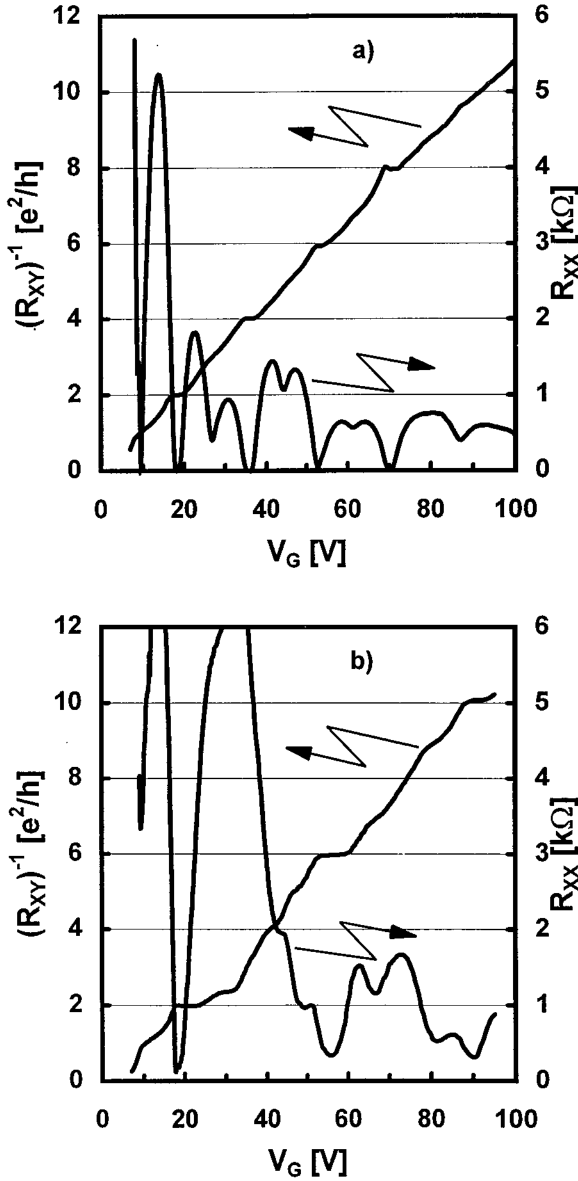

FIG. 3. Longitudinal resistance R_{xx} and Hall resistance R_{xy} as a function of gate voltage for stress $X=0$ kbar (a) and $X=5.1$ kbar (b), $X||[110]$.

force applied to the strings. At all stress values excellent reproducibility of the resistance changes was observed.

All the experiments were performed at $T=2.1$ K with the sample immersed in liquid helium. Gate voltages up to 200 V were applied by a ramp generator. The value of the dc drain current was 2 μA, low enough for avoiding distortions of the quantum Hall effect (QHE) plateaus. The quantities deduced were the longitudinal resistance R_{xx} and the Hall resistance R_{xy}. As the measuring field, 10.7 T was chosen where only the lowest subband of the [001] valley is populated at zero stress. The threshold voltage for the onset of conduction was 8 V and remained constant when applying stress and/or magnetic field.

IV. EXPERIMENTAL RESULTS

Figure 3 shows SdH and Hall effect data at zero stress and at 5.1 kbar. As the basis of a detailed discussion of the data in Sec. V the positions of the SdH minima are plotted in a

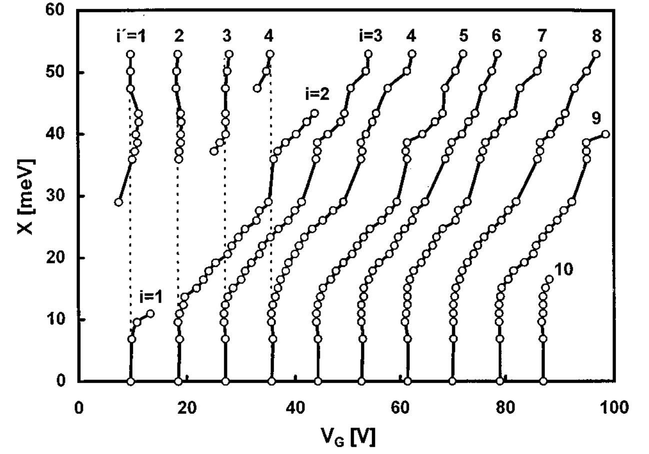

FIG. 4. Positions of the minima of the SdH oscillations as a function of applied stress X in [110] direction. The highest stress value is 6 kbar (conversion to meV see Fig. 2).

diagram of stress vs gate voltage. This is shown for stress $X||[110]$ in Fig. 4. A shift of the minima to higher V_G values is clearly observed above a certain stress applied. The minima of R_{xx} correspond to integer filling factors of Landau levels or Landau sublevels (spin and valley splitting taken into account). The actual values of the filling factors are obtained from the numbering of the minima and additionally from the R_{xy} values of the corresponding QHE plateaus. The periods of the SdH oscillations on the V_G scale vary with increasing stress. At the highest stress the period is 10% larger than at zero stress. At low V_G values the shifts of the minima (labeled by the filling factor i) in Fig. 4 are accompanied by the appearance of an additional set (labeled i') at high stress values. The i' minima occur at the same V_G values as the corresponding i minima (indicated by the dashed lines). For stress parallel to [100] qualitatively similar results are obtained (Ref. 18 and Fig. 5]. The quantitative

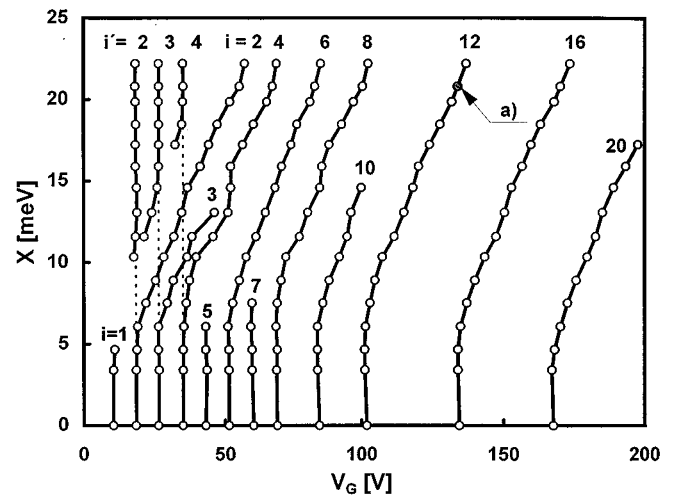

FIG. 5. Positions of the minima of the SdH oscillations as a function of applied stress X in [100] direction. The highest stress value is 2.5 kbar.

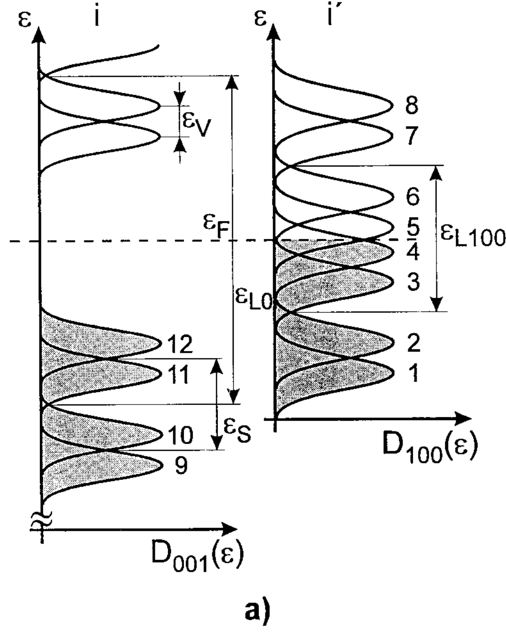

FIG. 6. Schematic energy-level structure at point a in Fig. 5. $D(\varepsilon)$ denotes the density of states in valleys as indicated; ε_F Fermi energy; ε_L, Landau splitting; ε_S, spin splitting; ε_V, valley splitting; $m_{001}=0.19m_0$; $m_{100}=0.42m_0$ (Ref. 12).

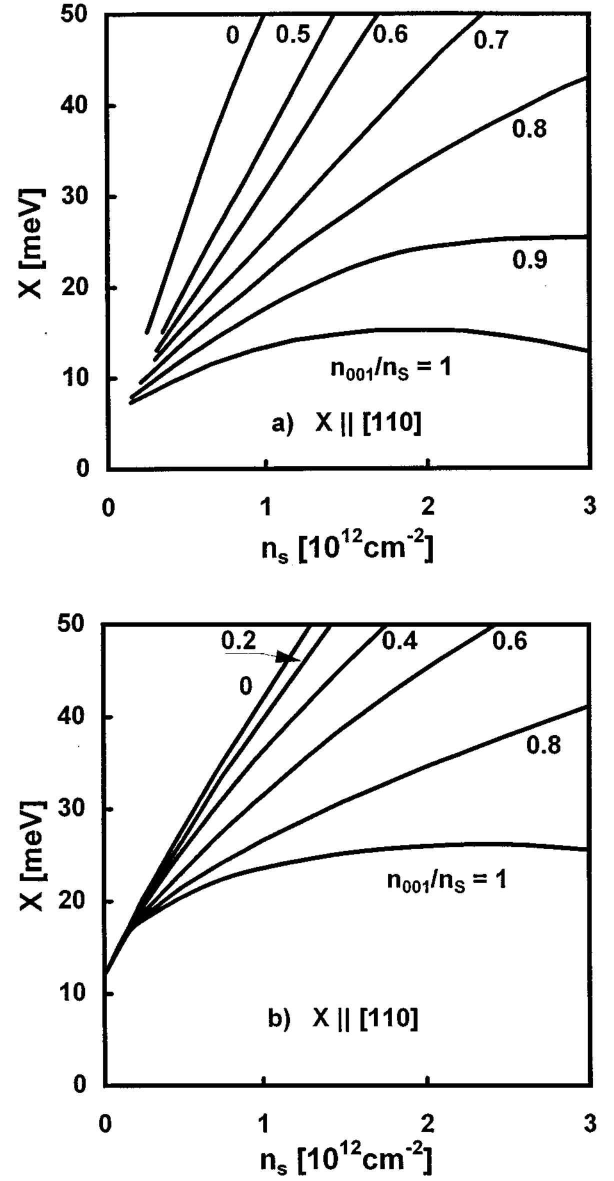

FIG. 7. (a) Experimentally determined phase diagram for the (001) MOSFET with $X||[110]$ direction. (b) Theoretical phase diagram after Takada and Ando, $n_{\rm dep}=1\times10^{11}$ cm^{-2} (Ref. 20).

differences are discussed in connection with the phase diagram in Sec. V. The broadening of the Hall plateaus at intermediate stress values is discussed in Ref. 19.

V. INTERPRETATION AND CONCLUSIONS

For the interpretation of the data it is assumed that the oxide capacitance and the threshold voltage do not change with stress. This is confirmed by the following experimental observations: The low-field Hall effect is independent of the stress. The minima with the same values of the filling factors i and i' appear at the same V_G values (Figs. 4 and 5) indicating no change of the carrier density. The measured threshold voltage is independent of the stress.

A. Energy-level scheme

Because of the many-valley structure the SdH data show minima not only according to the Landau-level structure and the spin splitting but also due to valley splitting. For example, for $X=0$ the minima at $V_G=36$ and 70 V in Fig. 4 correspond to Landau splitting (filling factor $i=4$ and 8, respectively), those at 53 and 86 V to spin splitting ($i=6$ and 10, respectively), those at 44 and 62 V to the valley splitting ($i=5$ and 7, respectively). Taking this into account, the energy-level structure of the subbands of the [001] and the [100] valleys can be deduced. Figure 6 shows the result for a representative situation in the [100] sample marked by a in Fig. 5. At $X=0$ and up to a certain stress value the [100] subbands are above the Fermi energy ε_F, which lies in the fourth Landau gap ($i=16$, $i'=0$) of the [001] subbands. At point a ($X=2.37$ kbar) also a total of 16 sublevels are filled, but with $i=12$ and $i'=4$ (Fig. 6). Increasing the stress further leads to the situation where only the [100] subbands are finally populated.

B. The phase diagram of valley occupations

The data of Figs. 4 and 5 are used to construct a phase diagram and to compare it with the theoretical results discussed in Sec. II B. If a minimum of set i is shifted to higher voltages from the voltage at $X=0$ it means that there are more electrons in the 2D layer than can be accommodated by this set; additional levels have to be populated as demonstrated by the appearance of the i' structure in Figs. 4 and 5. With increasing stress the electrons are transferred from the [001] (i set) to the [100] valleys (i' set) that become lower in energy. The shifts of the R_{xx} minima and their numbering together with the corresponding values of the quantized Hall resistance are a quantitative measure of the occupation of the two sets of subbands involved. On this basis the phase diagrams for $X||[100]$ and [110] are obtained and are plotted in Figs. 7 and 8. As can be seen from a comparison of Figs. 7 and 2 the RPA describes the experimentally obtained phase

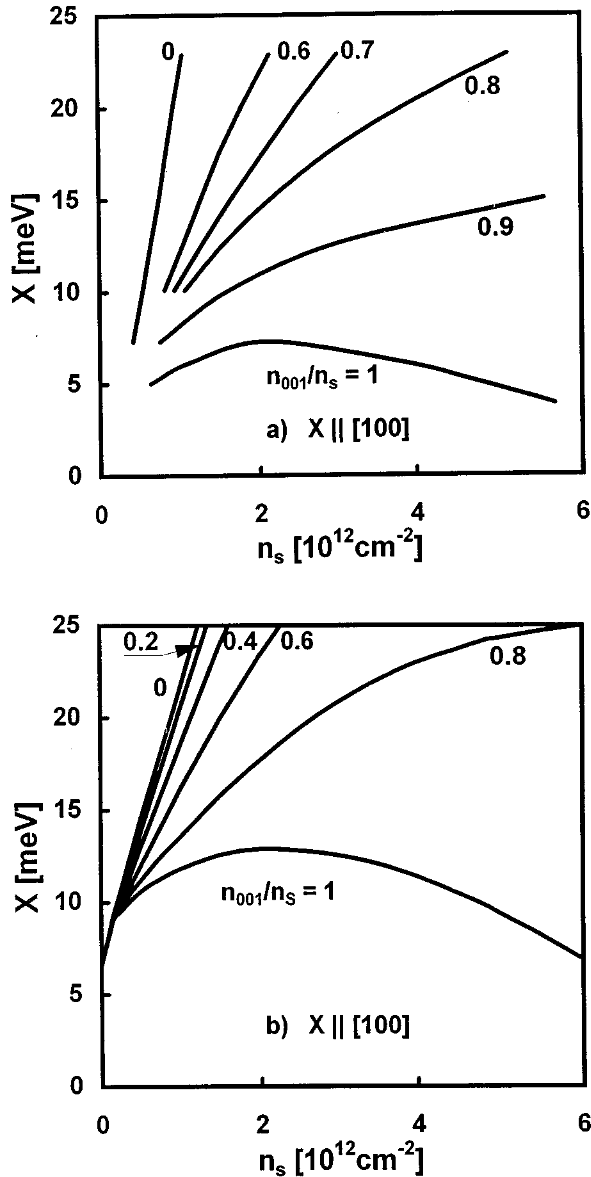

FIG. 8. (a) Experimentally determined phase diagram for the (001) MOSFET with uniaxial stress in the [100] direction. (b) Theoretical phase diagram, $n_{\rm dep} = 1\times10^{11}$ cm^{-2} (Ref. 6).

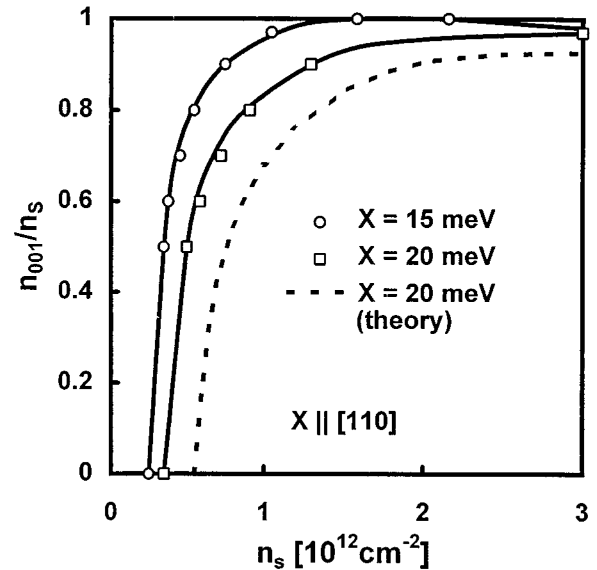

FIG. 9. Relative electron density of the [001] valleys as a function of the total electron density in the 2DES for two values of the stress in [110] direction. Solid curve, experiment; dashed curve, theory (Ref. 20).

diagram much better than the other approximations. Therefore, we also show the detailed RPA results of Takada and Ando[6,20] in Figs. 7(b) and 8(b).

In previous publications the experimental results of the magnetoresistance were considered as being in contradiction to the CR measurements[11] and to the theoretical results of Takada and Ando.[6] The main feature was a constant SdH period independent of stress without any indication of a second period of another valley. Our R_{xx} data, however, show that the SdH period for $V_G > 50$ V (i.e., $n_s > 1.5\times10^{12}$ cm^{-2}) actually increases with stress to a value 10% larger than without stress. Therefore we conclude that, as soon as valleys other than the [001] contain electrons, the stress-lowered valleys are pinned to the Fermi energy and the number of electrons in these valleys stays roughly constant. This could not be observed by Englert *et al.*[2] because of lower sample quality and weaker SdH oscillations. Only a constant period in R_{xx} and a change of the phase of the oscillations with increasing stress were detected. We, too, cannot observe a second period because in the V_G region, where we see clearly defined SdH oscillations, most of the electrons are in the [001] valleys and dominate the SdH oscillations. In regions where the numbers of electrons in different valleys are comparable only two or three periods of a SdH oscillation occur. Therefore, again two different periods cannot be resolved. But we observe a change of the SdH period with increasing stress as a consequence of the population of additional valleys.

This discussion already shows that a CDW-based interpretation is inconsistent with our experimental data. Additionally we observe a slow variation of n_{001} near $n_{001}/n_s = 1$ for $X||[110]$ (Fig. 9) as well as for $X||[100]$ in contradiction to the predictions of the CDW model.[5] There a first-order phase transition should occur at $n_{001}/n_s = 1$. Instead, near $n_{001}/n_s = 0$, Fig. 9 shows a very rapid variation of n_{001} consistent with the theoretical prediction.[20]

Our interpretation is based on a comparison of experiments in high magnetic fields and of a $B = 0$ theory. This procedure can be justified by taking into account the overlap of neighboring levels due to the broadened density of states of the Landau sublevels. For our samples and $B = 10.7$ T this overlap can be considered as being strong enough[1] to apply the $B = 0$ density of states as a good approximation in high fields. The observation of pronounced but narrow minima in R_{xx} has not been seen in contradiction since they are essentially caused by localization in the tails of the overlapping sublevels. The main effect of the magnetic field is the energetic shift of the ground state of the valleys. Because of the different masses in the different valleys this results in a shift of the whole phase diagram towards lower stress values. Considering this shift in the phase diagram the differences between the experimental and theoretical results for both stress directions are significantly reduced.

C. Valley degeneracy

As mentioned in Sec. II B an old problem of the physics of Si MOSFET's has been the observation of $g_v = 2$ regardless of the surface orientation. In this work we found that a valley degeneracy $g_v > 2$ can be realized. With stress in the [100] direction $g_v = 4$ occurs under conditions where the interplay of stress and electron-electron interaction allows us to establish a population of four valleys ($X > 1$ kbar and $V_G > 40$ V). For stress in the [110] direction again a condition can be realized ($X > 1.5$ kbar and $V_G > 40$ V) where valleys other than the [001] are also populated. However, it is not possible to decide between valley degeneracy 4 and 6 from our R_{xx} data because the V_G region at highest stress, where the electrons in the stress lowered valleys dominate the SdH oscillations, is too narrow. This might be possible with samples with much higher mobility and at higher stress values.

VI. SUMMARY

Our study of stressed Si MOSFET's has shown that the detailed features of the magnetotransport experiments are consistent with cyclotron resonance observations.[10,11] This allows us to exclude an interpretation on the basis of charge density waves.[5] Excellent agreement is found with theoretical results where the intervalley electron-electron interaction without involving phonons is considered.[6] A conclusion regarding the valley degeneracy is that $g_v > 2$ can be observed in magnetotransport measurements under appropriate strengths of the stress and the electron-electron interaction.

ACKNOWLEDGMENTS

The authors would like to thank Professor T. Ando and Professor Y. Takada for communicating unpublished results of the $X||[110]$ phase diagram and Dr. G. Dorda for the fabrication of the MOSFET's.

[1] Review by T. Ando, A. B. Fowler, and F. Stern, Rev. Mod. Phys. **54**, 437 (1982).
[2] Th. Englert, G. Landwehr, K. von Klitzing, and G. Dorda, Phys. Rev. B **18**, 794 (1978).
[3] G. Dorda, H. Gesch, and I. Eisele, Solid State Commun. **20**, 429 (1976).
[4] P. Stallhofer, J. P. Kotthaus, and J. F. Koch, Solid State Commun. **20**, 519 (1976).
[5] M. J. Kelly and L. M. Falicov, Phys. Rev. Lett. **37**, 1021 (1976); Phys. Rev. B **15**, 1974 (1977).
[6] Y. Takada and T. Ando, J. Phys. Soc. Jpn. **44**, 905 (1978).
[7] F. Stern and W. E. Howard, Phys. Rev. **163**, 816 (1967).
[8] I. Eisele, H. Gesch, and G. Dorda, Solid State Commun. **22**, 185 (1977).
[9] Th. Englert, G. Landwehr, J. Pontcharra, and G. Dorda, Surf. Sci. **98**, 427 (1980).
[10] P. Stallhofer, J. P. Kotthaus, and G. Abstreiter, Solid State Commun. **32**, 655 (1979).
[11] G. Abstreiter, P. Stallhofer, and J. P. Kotthaus, Surf. Sci. **98**, 413 (1980).
[12] H. Gesch, G. Dorda, and P. Stallhofer, Solid State Commun. **32**, 543 (1979).
[13] C. Herring and E. Vogt, Phys. Rev. **101**, 944 (1956).
[14] A. K. Ramdas and S. Rodriguez, Rep. Prog. Phys. **44**, 1297 (1981).
[15] M. J. Kelly and L. M. Falicov, Surf. Sci. **73**, 303 (1978).
[16] M. J. Kelly and W. Hanke, Phys. Rev. B **23**, 924 (1981).
[17] F. Kuchar, K. Veigl, and E. J. Fantner, Rev. Sci. Instrum. **50**, 245 (1979).
[18] J. Lutz, F. Kuchar, and G. Dorda, in *High Magnetic Fields in Semiconductor Physics II: Transport and Optics*, edited by G. Laudwehr, Springer Series in Solid State Sciences, Vol. 87 (Springer-Verlag, Berlin, 1989), p. 41.
[19] J. Lutz and F. Kuchar, Semicond. Sci. Technol. **11**, 1630 (1996).
[20] Y. Takada and T. Ando (private communication).